Neoplasma 2025; 72(6): 383–393

doi:10.4149/neo_2025_250917N396

Peroxisome proliferator-activated receptors as novel targets of small cell lung cancer circulating tumor cells

Gerhard HAMILTON[1,*], Marie-Therese EGGERSTORFER[1], Lukas WEIGL[2], Maximilian Johannes HOCHMAIR[3], Sandra STICKLER[1]

[1]*Institute of Pharmacology, Medical University of Vienna, Vienna, Austria;* [2]*Department of Special Anesthesia and Pain Therapy, Medical University of Vienna, Vienna, Austria;* [3]*Karl Landsteiner Institute for Lung Research and Pulmonary Oncology, Hospital Floridsdorf, Vienna, Austria*

**Correspondence: gerhard.hamilton@meduniwien.ac.at*

Received September 17, 2025 / Accepted November 6, 2025

Small cell lung cancer (SCLC) has a dismal prognosis with a low 2-year survival rate. Chemotherapy for recurrent SCLC fails invariably, and novel tumor targets are needed. Here, the effects of agents targeting the peroxisome proliferator-activated receptors (PPARs) in SCLC are investigated. Initial screening of 96 PPAR-directed agents was performed in two SCLC CTC-derived lines (BHGc10, BHGc16). Compounds showing high cytotoxicity were subsequently tested in two pleural effusion-derived lines (S457, S1392) and the SCLC line NCI-H69. Several PPARs emerged as actionable targets: eight PPARγ ligands and nine ligands for PPARα, PPARα/δ, or PPARβ/δ. For the six most effective compounds, treatment-induced protein changes were further profiled in BHGc16 using protein arrays. Cytotoxicity varied by compound, while the PPARγ agonist pioglitazone and the PPARα agonist fenofibrate were preferentially active in CTC lines, DG172 hydrochloride was selective for pleural effusion-derived lines, while rosiglitazone maleate, cloxiquine, and agrimol B showed no selectivity. Mechanistically, in the CTC-derived cell line BHGc16, these six PPAR-directed agents increased pro-apoptotic proteins (Bax, Bad, caspase-3/9), decreased anti-apoptotic and invasion proteins (Bcl-2, Bcl-XL, c-FLIP-L, ICAM-1, CXCR4), and suppressed Akt/mTOR, MEK/ERK, p38 MAPK, and JAK2/STAT3 signaling. These findings support PPARs as clinically relevant targets in SCLC, with PPAR-directed agents showing cytotoxic effects comparable to those reported in other malignancies. Such agents may aid SCLC treatment and help delineate biological differences between CTCs and resident tumor cells.

Key words: small cell lung cancer; circulating tumor cells; peroxisome proliferator-activated receptor; cytotoxicity

Peroxisomes are intracellular structures present in the majority of animal cells, involved in metabolic processes such as hydrogen peroxide-based respiration, fatty acid (FA) beta-oxidation, and cholesterol metabolism [1, 2]. Transcriptional regulators controlled by FAs lead to alterations of the size and number of peroxisomes present [3]. Alternatively, chemically unrelated peroxisome proliferators (PPs) can replace FAs in their effects on peroxisomes. The function of PPs is mediated by specific receptors, known as peroxisome proliferator-activated receptors (PPARs), which belong to the nuclear receptor superfamily. PPARs consist of three genetically homologous isotypes, namely PPARα, γ, and β/δ, that are key metabolic regulators of the body [4]. Besides the involvement in nutrient and energy metabolism, they control lipid and carbohydrate turnover, cell growth, and cancer development [5]. After ligand binding, PPARs bind to peroxisome proliferation reaction elements (PPREs) on the DNA and, after heterodimerization with retinol X receptors (RXR), this complex regulates the transcription of target genes in the nucleus [6, 7]. Activated PPARs may additionally exert DNA-independent transcriptional repression of transcription factors such as NFκB, STAT-1, and AP-1 signaling factors. The endogenous ligands of PPARs are mostly FAs and their derivatives [8]. PPAR ligands are regarded as potential anticancer agents with relatively low systemic toxicity [9]. PPARα activation can target cancer cells' energy balance by blocking FA synthesis and by promoting β-oxidation. PPARα can divert energy metabolism toward FA degradation and decrease glucose uptake by inhibiting glucose transporter GLUT4 [10, 11]. PPARα activation leads to the upregulation of enzymes involved in FA uptake, transport to mitochondria, and subsequent oxidation. This enhances the break-

down of FAs when glucose availability is limited and energy is required. PPARβ/δ activation is associated with tumor progression, whereas PPARα and PPARγ activation may be associated with tumor suppression. In the repressed state, the PPAR/RXR heterodimer binds to corepressor proteins, containing histone deacetylase activity, and eventually turns down target gene transcription [12]. Upon ligand binding, the heterodimer releases the corepressor, enhancing the coactivator activity [13].

Antitumor effects of the PPARα, PPARβ/δ, and PPARγ ligands were reported frequently [14, 15]. In detail, inhibition of PPARα reduces cell migration and increases cell death in malignant cells. Mechanisms discussed include the downregulation of Myc, delayed G0/G1 phase transit, and the downregulation of cyclin-dependent kinases (CKs), respectively. Furthermore, activation of PPARγ retards the proliferation of a glioblastoma cell line and is followed by apoptosis [16]. PPARα (e.g., clofibrate) and PPARγ agonists (e.g., pioglitazone) suppress the tumor growth, decrease angiogenesis, and promote apoptosis [17]. The PPARα agonists, fenofibrate and bezafibrate, were found to exert chemopreventive activity [17]. Fenofibrate impairs IGF-IR signaling, resulting in increased reactive oxygen species (ROS), lower ATP production, and damaged mitochondria [18]. In cancer, PPARs disturb the activity of phosphatases and kinases, including ERK1/2, p38-MAPK, PKC, AMPK, and GSK3. PPARγ is frequently expressed in tumor cells, and its activation leads to either inhibition of cell growth or induction of cell death [19, 20]. Although each PPAR either suppresses or promotes tumor progression, depending on the specific tumor or ligands, the mechanisms are still largely unclear [21]. Of special interest is the potential inhibitory effect of PPARγ ligands on the metastatic potential of cancer cells [22, 23]. In this respect, the thiazolidinediones (TZDs) class of synthetic ligands for PPARγ, including rosiglitazone, pioglitazone, and others, which are commonly used to lower blood sugar, have been studied so far [24, 25]. Pioglitazone targets PPARγ-regulated genes and strongly reduces cell invasiveness in addition to anti-proliferative effects in various malignancies. Normal cells appear to be largely insensitive to pioglitazone application [26, 27]. In general, PPAR*γ* agonists hinder cancer cells' migratory and invasive capabilities for successful metastasis [23]. Angiogenesis and the expression of matrix metalloproteinases and extracellular matrix (ECM) proteins seem to be modulated by PPAR*γ* in the tumor microenvironment.

In the present study, PPAR-directed agents active against small cell lung cancer (SCLC) and circulating tumor SCLC cell lines (SCLC CTC) were detected in a screen of a compound library comprising over 700 transcription factor (TF) inhibitors. SCLC accounts for 15–20% of lung cancers, and the majority of patients show tumor dissemination at first presentation [28]. SCLC exhibits exceptionally large numbers of CTCs that enabled our lab to establish a panel of permanent SCLC CTC lines that proved tumorigenic in mice and thus have metastasis-inducing capabilities [29, 30]. With the help of these cell lines, the effects of PPAR-directed agents on metastasis-mediating SCLC tumor cells could be checked in a direct manner, and furthermore, pleural effusion-derived SCLC lines were tested for comparison. CTCs were reported for most tumor entities, although at low numbers, and are different from SCLC by a lack of derived cognate long-term tumor cell lines [31].

Materials and methods

Cell lines. The SCLC cell line NCI-H69 was acquired from the American Type Culture Collection (HTB-119, ATCC, Manassas, VA, USA). The SCLC CTC lines BHGc10 and BHGc16 were obtained from blood samples, and the SCLC cell lines S457 and S1392 were pleural effusion-derived and were successfully established at our laboratory. Samples were obtained from relapsed SCLC patients before second-line chemotherapy. All SCLC cell lines belonged to the SCLC-A subtype, except for the SCLC-P line S1392, as confirmed by RNA sequencing, with gene expression values normalized to transcripts per million (TPM) (Supplementary Table S1). Pleural effusions are routinely obtained from SCLC patients since their removal is a necessary means to improve breathing for patients. All clinical specimens were obtained from patients with informed consent and according to the guidelines of the Ethics Approval 366/2003 granted by the Ethics Committee of the Medical University of Vienna, Vienna, Austria.

Cell culture. For cell culture in 75 cm^2 tissue culture flasks (#658170, Greiner Bio-One GmbH, Kremsmünster, Austria) the cells were kept in culture medium RPMI-1640 medium (#R8758, Sigma-Aldrich, St. Louis, MO, USA) supplemented with 10% fetal bovine serum (FBS) (#SFBS-AU, Eximus, Catus Biotech, Tutzing, Germany) and antibiotics (#P4458, Sigma-Aldrich, Darmstadt, Germany). All cells were kept under tissue culture conditions of 37°C at 5% CO_2 and regularly split by replacement of medium. All cells were harvested by pipetting, except for tuft-like S1392 that attaches loosely and can be released with cell scrapers or pipetting. Cells were counted with a LUNA automated cell counter (Biozym, Vienna, Austria).

Compounds. All compounds were used as 10 mM stock solutions in dimethyl sulfoxide (DMSO). Samples were obtained as part of the Transcription Factor Library L1380 (Batch #PHD156583), comprising 704 compounds (Targetmol, Welesely Hills, MA, USA). Due to the aim of this study, the focus was on 96 agents linked to PPAR, some of which modulate it in an indirect manner (Supplementary Table S2).

MTT cytotoxicity assays. To obtain the half-maximal inhibitory concentration values (IC_{50} values) of the compounds, 1×10^4 cells in 100 µl complete RPMI-1640 medium (supplemented with 10% FBS and antibiotics) were distributed to the wells of 96-well flat-bottom microtiter

plates (92096, Techno Plastic Products AG, TPP, Trasadingen, Switzerland). Two-fold dilutions of test compounds were added in triplicate, while assays were also performed at least in triplicate. After four days of incubation under tissue culture conditions, viable cells were detected at 450 nm using a modified 3-(4,5-dimethylthiazolyl-2)-2,5-diphenyltetrazolium bromide (MTT) assay (EZ4U, Biomedica, Vienna, Austria). IC_{50} values were calculated from dose-response curves evaluated via Origin 9.1. software (OriginLab, Northampton, MA, USA). Initial screening encompassed testing of all 96 compounds on BHGc10 and BHGc16. Thereafter, if IC_{50} values below 9 µM were achieved, these compounds were further tested in all other cell lines.

Proteome profiler oncology XL arrays. Relative expression of oncology-related proteins in BHGc16 treated with pioglitazone, rosiglitazone maleate, cloxiquine, fenofibrate, agrimol B, and DG172 dihydrochloride was determined using a Proteome Profiler Human Oncology XL Array Kit (#ARY026, R&D Systems, Minneapolis, MN, USA) according to the manufacturer's instructions. The cancer cells were lysed using the lysis buffer 17 (#895943, R&D Systems) according to the supplied instructions. Experiments were performed in duplicate, and the six reference spots provided on each membrane were used to calibrate the individual chemiluminescence intensities. The arrays were evaluated using Quickspot (Ideal Eyes System, Bountiful, UT, USA) and Origin 9.1 software.

Statistical analysis. We aimed to find differences in the expression of cancer-related proteins between control and six different treatments. Therefore, we conducted repeated measures ANOVAs for control and treatment comparisons of Proteome Profiler Human Oncology XL Array data. Normality was evaluated via a Shapiro-Wilk test and sphericity via a Mauchly's Test for Sphericity. Analysis was conducted using Origin 9.1. software (OriginLab, Northampton, MA, USA).

Results

Cytotoxicity assays of PPAR-directed agents. A range of PPAR-directed agents was tested in chemosensitivity assays in 6 two-fold dilution steps starting with a 20 µM concentration (Supplementary Tables S2, S3). Pioglitazone showed similar dose-dependent activity against the SCLC CTC lines BHGc10 and BHGc16, whereas the pleural effusion-derived S457 cells showed lower sensitivity. Cloxiquine exhibited cytotoxic activity against all three cell lines, BHGc10 and BHGc16 SCLC CTCs, as well as against S457 cells;

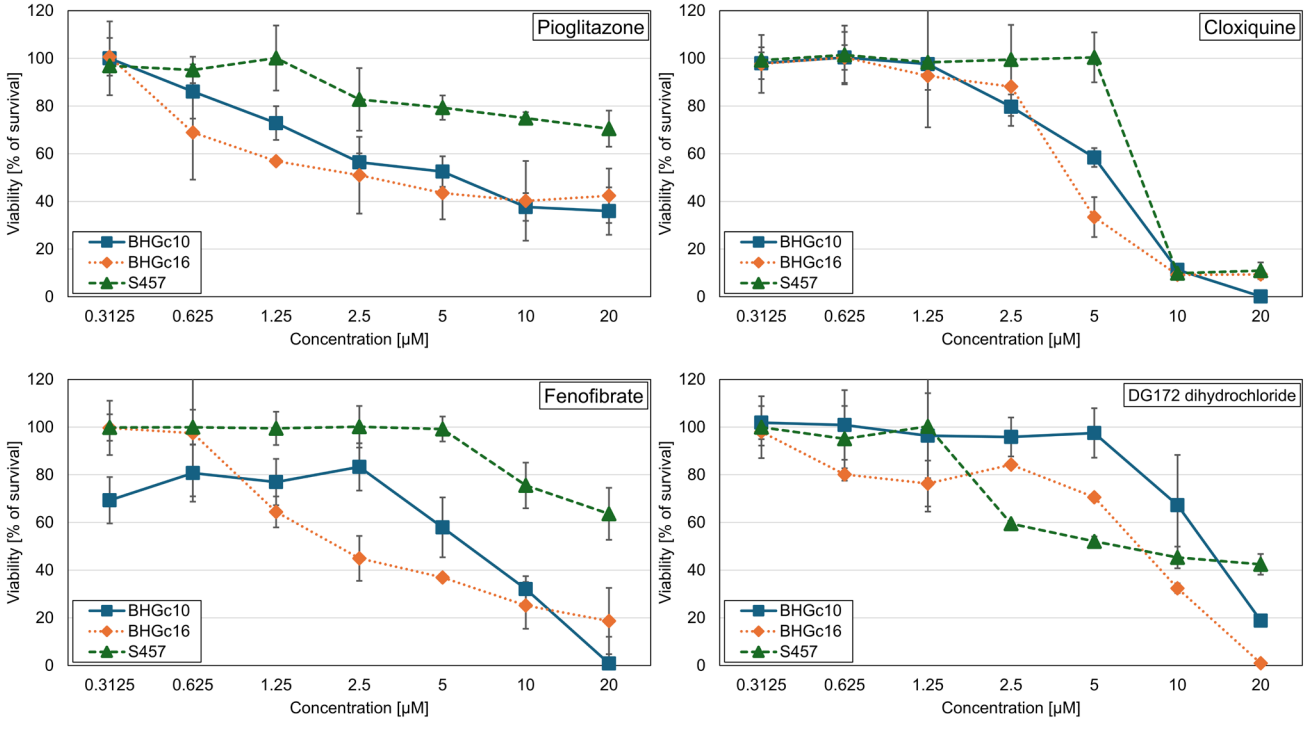

Figure 1. MTT cytotoxicity assays of the cell lines treated with pioglitazone, cloxiquine, fenofibrate, and DG172 dihydrochloride. Data shown are mean values ± SD for 6 two-fold dilutions of the compound starting at 20 µM. IC_{50} values of pioglitazone were 5.89 µM for CTC cell line BHGc10 and 2.7 µM for CTC cell line BHGc16, respectively. No IC_{50} value could be achieved for the SCLC cell line S457 due to the low cytotoxicity of the compound in this cell line. IC_{50} values for cloxiquine were 5.89 µM for BHGc10, 4.29 µM for BHGc16, and 7.77 µM for S457, respectively. IC_{50} values for fenofibrate were 6.40 µM for BHGc10 and 2.19 µM for BHGc16, respectively. No IC_{50} value could be achieved for S457 due to the low cytotoxicity of the compound in this cell line. IC_{50} values for DG172 dihydrochloride were 13.52 µM for BHGc10, 7.86 µM for BHGc16, and 6.20 µM for S457, respectively.

however, with a relatively lower potency. Fenofibrate showed high cytotoxic activity against BHGc16 cells, considerable activity against BHGc10 cells, but failed to exert significant cytotoxic effects on the pleural effusion-derived S457 cells. In contrast, DG172 hydrochloride showed higher cytotoxic activity against S457 cells with lower potency on BHGc16 and especially BHGc10 cells (Figure 1).

Summary of cytotoxicity tests of PPAR-directed agents. Data for the PPARγ-directed drugs are summarized in Figure 2. Mean IC_{50} values are shown for pioglitazone, rosiglitazone maleate, and cloxiquine as found in MTT tests employing the two SCLC CTC lines, the NCI-H69 SCLC cell line, and two pleural effusion-derived SCLC lines, S457 and S1392. While pioglitazone was active against both SCLC CTC lines, rosiglitazone maleate was cytotoxic for the BHGc16 line, and cloxiquine was cytotoxic for all cell lines tested.

Data for other PPAR-directed drugs are summarized in Figure 3. Mean IC_{50} values are shown for fenofibrate, agrimol B, and DG172 hydrochloride as found in MTT tests employing the two SCLC CTC lines, the NCI-H69 SCLC cell line, and two pleural effusion-derived SCLC lines, S457 and S1392. While fenofibrate was active against both SCLC CTC lines, agrimol B was cytotoxic for all cell lines tested, and DG172 hydrochloride showed preferential activity for the pleural effusion-derived SCLC cell lines in contrast to the BHGc16 and BHGc10 SCLC CTC cell lines. The H69 cell line was resistant to pioglitazone, rosiglitazone maleate, and fenofibrate, sensitive to cloxiquine and agrimol B, and highly sensitive to DG172 hydrochloride.

Changes in protein expression in response to PPAR agents. Alterations in oncology-related proteins in response to selected PPAR-directed agents were analyzed using Proteome Profiler XL western blot arrays that capture 84 proteins. The proteins exhibiting the largest effects of the PPAR-directed compounds of the BHGc16 SCLC CTC line are shown in Figures 4A and 4B for 6 active compounds. The PPAR agents were used at their IC_{50} concentrations (Supplementary Tables S2, S3) for an incubation period of two days. Proteins showing significant changes in expression compared to controls are indicated by asterisks (statistical data available in Supplement A and B). In general, proteins involved in apoptosis, protein degradation, cell proliferation, and cell adhesion are targets of the PPAR-directed agents.

Pioglitazone resulted in an upregulation of BCL-X and downregulation of ErbB3/HER3, Enolase 2, EpCAM, p27/Kip1, Serpin B5/Maspin, and Survivin. Rosiglitazone maleate also led to an upregulation of BCL-X; however, in line with CapG and Cathepsin S and downregulation of ErbB3/HER3, Enolase 2, EpCAM, p27/Kip1, Serpin B5/Maspin, and Survivin. Cloxiquine downregulated BCL-X,

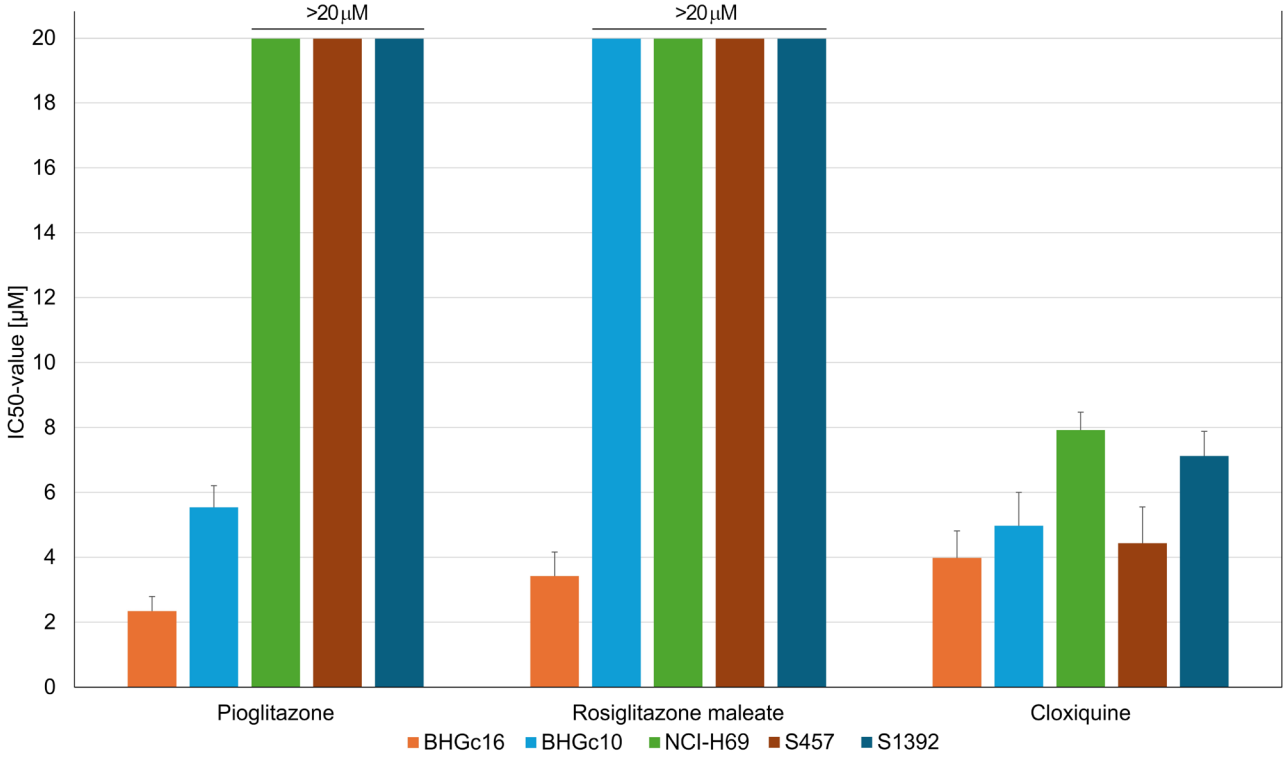

Figure 2. IC_{50} values for CTC and SCLC cell lines treated with pioglitazone, rosiglitazone maleate, and cloxiquine. Each PPAR-γ-directed compound was tested in triplicate (n=3) for each cell CTC cell line (BHGc16, BHGc10) and SCLC cell line (NCI-H69, S457, and S1392). Data shown are mean values ± SD. Bars ending at 20 µM indicate that no IC_{50} value could be reached up to 20 µM.

Cathepsin S, DLL1, ErbB3/HER3, p27/Kip1, Serpin B5/Maspin, and Survivin. Fenofibrate resulted in an upregulation of CapG and downregulation of ErbB3/Her3, Enolase 2, and Survivin. Agrimol B downregulated BCL-X, Cathepsin S, DDL1, ErbB3/Her3, Serpin B5/Maspin, and Survivin, and upregulated CapG and p27/Kip1. DG172 dihydrochloride also led to a downregulation of BCL-X and Survivin while upregulating Cathepsin S, ErbB3/Her3, and EpCam/TROP1.

Discussion

Reprogramming of cancer cell metabolism changes the metabolism of lipids and FAs to increase invasiveness, metastasis, and chemoresistance [1]. These variations in FA metabolism are put into execution by peroxisomes, and increased rates of FA oxidation accompany the progression of cancers in the liver, lung, and breast [32, 33]. PPAR agonists have been used in clinical practice for various indications. PPARγ agonists, such as TZDs, first reported as insulin sensitizers in the early 1980s, reduce blood glucose levels [20, 34, 35]. Generally, synthetic ligands regulate the transcription activation of PPARγ by completely displacing natural/endogenous ligands or by co-binding [36]. Full agonist TDZs have insulin-sensitizing effects, but antagonists such as GW9662 suppress the transcription of PPARγ-responsive genes by competitively binding with agonists [37]. PPARα agonists, such as fibrates, are used clinically to lower lipids [7]. PPARβ/δ activation can regulate HDL cholesterol levels and improve glycemic control [38].

Increased FA oxidation depletes levels of nicotinamide adenine dinucleotide phosphate (NADPH) and suppresses lung cancer growth by an adverse intracellular redox milieu [39]. The PPARγ agonist troglitazone, in combination with trimetazidine, increased FA oxidation in lung cancer, resulting in apoptosis [40]. Fenofibrate-mediated IGF-IR inhibition with PPARα-dependent metabolism generated ROS that suppressed glioma cell spread and survival of medulloblastoma cell lines [18, 41]. PPARγ agonists act synergistically with chemotherapy, but the clinical application of PPARγ agonists remains limited due to adverse side effects [23, 42]. Apart from the inhibition of tumor growth, studies have demonstrated that PPARγ activation exerts anti-tumor effects in lung cancer by inhibition of invasion and migration [43, 44]. In colon cancer, PPARα promoted metastasis by impairing the expression of Cox-2, VEGF, and matrix metalloproteinase (MMP)-9 [45, 46]. Pioglitazone suppressed pro-metastatic IL-8 and COX expression *in vitro* in pancreatic cancer cells [47].

During screening of a TF-directed compound library on SCLC and SCLC CTC cell lines, a range of PPAR-directed

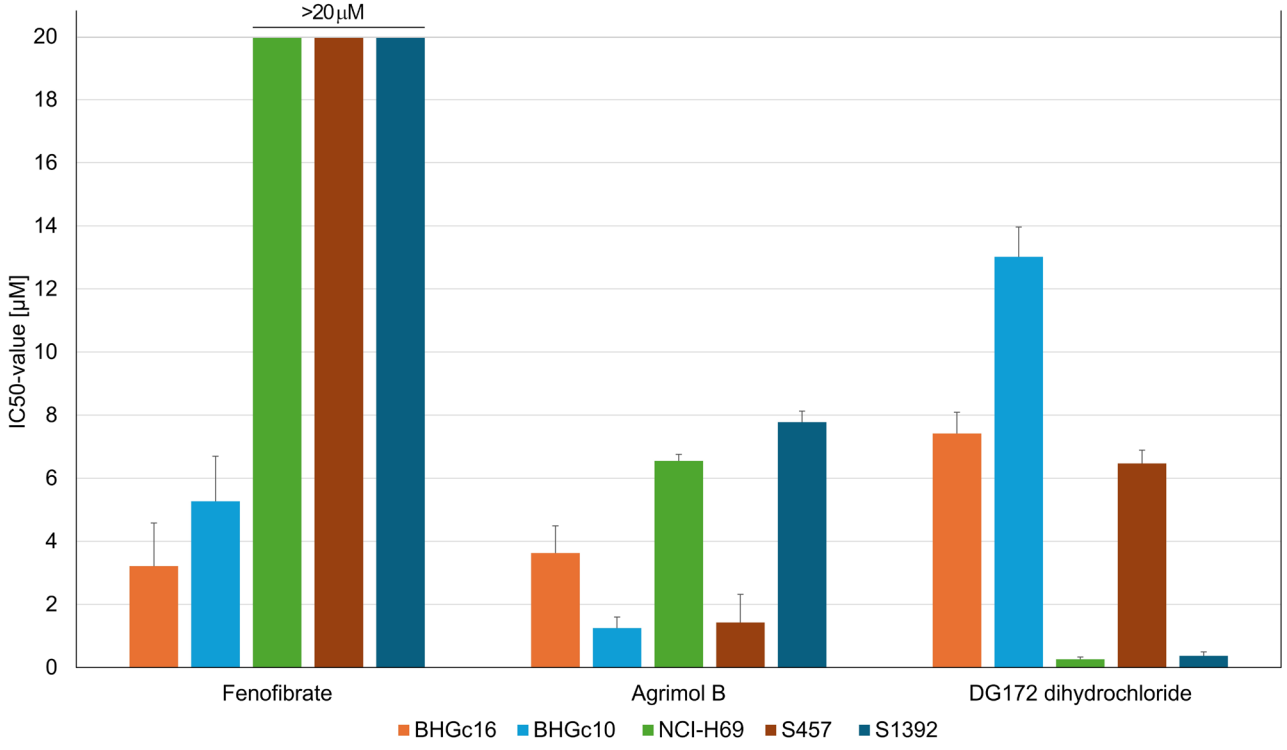

Figure 3. IC_{50} values for CTC and SCLC cell lines treated with fenofibrate, agrimol B, and DG172 dihydrochloride. Data shown are mean values ± SD. The PPARα-directed agent fenofibrate, the PPAR-γ-directed agent agrimol B, and the PPAR-δ/γ-directed agent DG172 dihydrochloride were each tested in triplicate (n=3) for each CTC cell line (BHGc16, BHGc10) and SCLC cell line (NCI-H69, S457, and S1392). Bars ending at 20 µM indicate that no IC_{50} value could be reached up to 20 µM.

agents were detected, and selected drugs were used for further characterization. With the exception of NCI-H69, the SCLC lines used were established from pleural effusions, and the SCLC CTC lines from blood samples of patients with advanced disease [29, 48]. This panel of SCLC cell lines is unique and truly represents metastasis-inducing tumor cells. Here, cytotoxicity tests showed that pioglitazone impairs both SCLC CTC lines in concentrations that can be achieved in patients but spared the pleural effusion-derived cell lines [49]. Rosiglitazone maleate inhibited only BHGc16 SCLC CTCs and spared the pleural effusion-derived lines. Fenofibrate exhibited a similar preference for the SCLC CTC cell lines as pioglitazone, but cloxiquine showed activity against all 5 SCLC lines. Agrimol B showed no clear preference, and DG172 was more active against the pleural effusion-derived cell lines compared to the SCLC CTC lines. Except for DG172, the tested compounds revealed low activity against the NCI-H69 cell line.

The protein changes induced by the range of active PPAR-directed agents were analyzed with the help of western blot arrays. Pioglitazone and rosiglitazone maleate downregulated ErbB3 and Enolase 2, besides alterations in proteases and p27/Kip1. In contrast, although cloxiquine revealed modifications of the same proteins, downregulation of

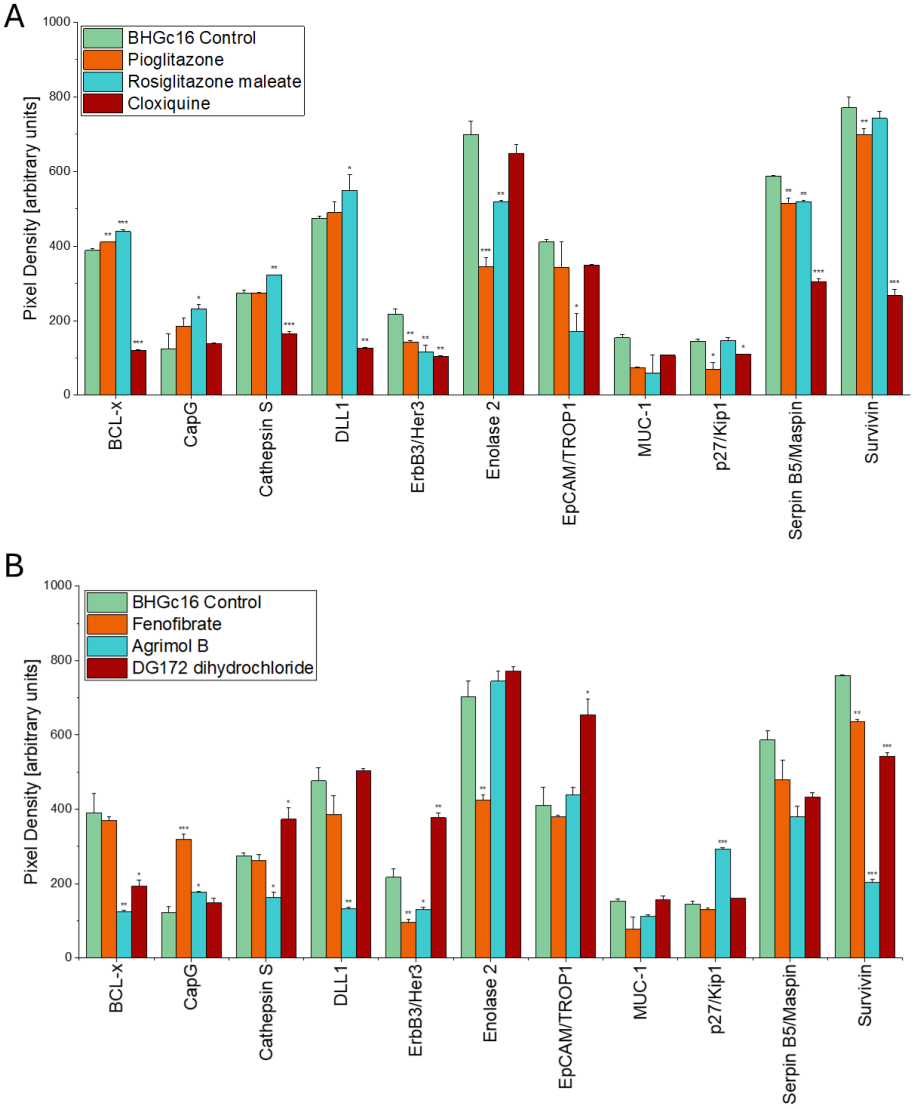

Figure 4. Protein expression changes in BHGc16 cells after treatment with PPAR modulators. This analysis of cancer-related proteins in BHGc16 control was conducted before and after treatment with A) pioglitazone, rosiglitazone, cloxiquine, and B) fenofibrate, agrimol B, and DG172 dihydrochloride. Data represent mean values ± SD, significant p-values are shown by an asterisk and indicate the difference of control to each group as evaluated by a repeated measures ANOVA (*p<0.05, **p<0.01, ***p<0.001). Abbreviations in the figure are as follows: BCL2 Like 1 (BCL-X), Capping Actin Protein Gelsolin Like (CapG), Delta Like Canonical Notch Ligand 1 (DLL1), Erb-B2 Receptor Tyrosine Kinase 3 (ErbB3/Her3), Epithelial Cell Adhesion Molecule (EpCAM/TROP1) and Cyclin Dependent Kinase Inhibitor 1B (p27/Kip1/CDKN1B).

BCL-X and Survivin points to the induction of apoptotic cell death. Downregulation of DLL1 expression in the cells results in an anti-oncogenic effect through its impairment of Notch signaling [50]. Fenofibrate showed a similar range of protein alterations with the replacement of MUC-1 by EpCAM and Survivin downregulation. Essentially the same list of modified proteins is apparent in BHGc16 in response to treatment with agrimol B and DG172.

A range of 10 other PPAR-directed agents with various activities against the SCLC lines are listed in Supplement 1. GW9662 binds to the PPARγ as an irreversible antagonist and inhibits adipocytic differentiation and, furthermore, suppresses the growth of breast cancer cell lines and glioblastoma stem cells [37, 51–53]. This compound was cytotoxic for all cell lines used, except for BHGc10. T0070907 is an effective and highly specific PPARγ inhibitor, with >800-fold selectivity over PPARα and PPARδ, that BHGc10 cells again showed resistance to [34]. The potent and selective PPARγ inhibitor SR1664 has antidiabetic activity and inhibits Cdk5-mediated PPARγ phosphorylation without exhibiting PPARγ agonist activity. Among the cell lines tested, this compound revealed activity limited to BHGc16. SR16832 constitutes a dual-site PPARγ inhibitor that prevents the binding of endogenous ligands and the transcriptional activity of PPARγ with preferential cytotoxicity for the pleural effusion-derived SCLC cell lines [54]. GW6471 is an antagonist of PPARα with IC_{50} of 0.24 μM that showed cytotoxic activity except for SCLC S1392 [34]. MA-0204 is a highly selective and orally available PPARδ modulator with anticancer activity, and its activity is restricted to BHGc16 [21]. The selective PPARβ/δ antagonist CC618 showed variable activity against the SCLC cell lines, while BHGc10 cells revealed resistance against the anti-diabetic PPARα modulator fucosterol. The CDDO-Im (TP-235) activator of PPARγ and Nrf2 exhibited high activity against the whole panel of SCLC cell lines and breast cancer cells [55]. The PPARγ-directed agents either showed activity against the SCLC CTC lines and lacked cytotoxicity for the pleural effusion-derived lines and NCI-H69 or exhibited activity for all lines tested. There is no clear correlation between the PPAR subtype targeted and the distribution of cytotoxicity against the SCLC and SCLC CTC cell lines.

Our results are in line with previous reports dealing with cancer cell lines different from SCLC. PPARγ activation increases pro-apoptotic factors Bax and Bad, decreases anti-apoptotic factors Bcl-2 and Bcl-XL, and promotes apoptosis through caspase3/9 activity and mitochondrial cytochrome c release [5, 56, 57]. Rosiglitazone-mediated PPARγ activation inhibits NSCLC cell proliferation via downregulation of the Akt/mTOR/p70S6K signaling cascade and triggers apoptotic cell death via generation of ROS [58, 59]. PPARγ activation could also suppress the expression of invasion-related proteins, such as intercellular adhesion molecule-1 (ICAM-1) and C-X-C chemokine receptor type 4 (CXCR4) [60, 61].

TZDs have been shown to inhibit the growth of liposarcoma, breast, colon, prostatic, gastric and pancreatic cancer [62–65]. Pioglitazone treatment resulted in the inhibition of proliferation and metastasis in human pancreatic cancer cells [47, 66]. Pioglitazone mediates apoptosis in Caki cells via downregulation of the caspase regulator c-FLIP-L and reducing Bcl-2 protein stability [65]. Furthermore, it inhibits the signal transducer and activator of transcription 3 (STAT3), MEK/ERK, p38 MAPK, BCL-2, and JAK2/STAT3 signaling pathways [67, 68]. Rosiglitazone is an orally active thiazolidinedione with antidiabetic properties and potential antineoplastic activity [69]. Cloxiquine, an antituberculosis drug, markedly suppresses the growth and metastasis of melanoma cells through PPARγ without apparent toxicity in normal melanocytes and in the liver. [70]. Agrimol B suppresses adipogenesis through modulation of the SIRT1-PPARγ signaling pathway [71]. Fenofibrate is a PPARα agonist that exhibits antihyperlipidemic activity and antitumor activity [72, 73]. DG-172 dihydrochloride is an antagonist of PPARβ/δ that inhibits cancer cell invasion [74]. A retrospective analysis of 87,678 male diabetics demonstrated that TZD users showed a 33% lower risk of lung cancer compared to non-users [22]. Diabetes was not significantly associated with lung cancer incidence (140,395 participants), and there were no significant associations between diabetes and lung cancer risk [75]. The 1-, 2-, and 3-year survival of non-diabetic versus diabetic patients with lung cancer were 43% vs. 28%, 19% vs. 11%, and 3% vs. 1%, respectively. Adjusted for other parameters in the Cox regression model, the hazard ratio for survival in diabetic patients with lung cancer was 0.55 (95% CI, 0.41–0.75) [76]. These findings may be explained by the inhibition of tumor dissemination in diabetic patients by PPAR-directed drugs or direct and indirect metabolic effects.

The lipidome of malignant lung pleural effusions exhibits a unique metabolic signature that can be used to discriminate benign disease [77, 78]. Thus, the pleural effusion-derived cell lines S457 and S1392 may be adapted to such special microenvironmental conditions. The CTCs seem to be released by leaky vessels in the core of the tumors and adapt to the conditions in the peripheral circulation to eventually generate secondary lesions [79, 80]. The knowledge of the biological characteristics of CTCs is incomplete, and the specific responsiveness to PPAR-directed agents may provide the opportunity to find new targets and novel modes of treatment in the case of SCLCs.

In summary, several PPAR-directed agents impair the proliferation and viability of SCLC CTC cells and may provide a valuable contribution to the therapy for this malignancy, with a survival rate below 2 years for advanced disease.

Supplementary information is available in the online version of the paper.

Acknowledgments: This study was not supported by any sponsor or funder.

References

[1] PRATAMA AM, SHARMA M, NAIDU S, BÖMMEL H, PRABHUSWAMIMATH SC et al. Peroxisomes and PPARs: Emerging role as master regulators of cancer metabolism. Mol Metab 2024; 90: 102044. https://doi.org/10.1016/j.molmet.2024.102044

[2] DAHABIEH MS, DI PIETRO E, JANGAL M, GONCALVES C, WITCHER M et al. Peroxisomes and cancer: The role of a metabolic specialist in a disease of aberrant metabolism. Biochim Biophys Acta 2018; 1870: 103–121. https://doi.org/10.1016/j.bbcan.2018.07.004

[3] ABDELMAK S, YANG N, RAY SD. Peroxisome proliferators, pp. 399–407. In: WEXLER P (Ed.). Encyclopedia of Toxicology (Fourth Edition). Academic Press, Elsevier, 2023, p. 399–407. ISBN 9780323854344. https://doi.org/10.1016/B978-0-12-824315-2.00218-9

[4] SUN J, YU L, QU X, HUANG T. The role of peroxisome proliferator-activated receptors in the tumor microenvironment, tumor cell metabolism, and anticancer therapy. Front Pharmacol 2023; 14: 1184794. https://doi.org/10.3389/fphar.2023.1184794

[5] KIM TW, HONG DW, HONG SH. CB13, a novel PPARγ ligand, overcomes radio-resistance via ROS generation and ER stress in human non-small cell lung cancer. Cell Death Dis 2020; 11: 848. https://doi.org/10.1038/s41419-020-03065-w

[6] PHUA WWT, WONG MXY, LIAO Z, TAN NS. An aPPARent functional consequence in skeletal muscle physiology via peroxisome proliferator-activated receptors. Int J Mol Sci 2018; 19: 1425. https://doi.org/10.3390/ijms19051425

[7] TAN Y, WANG M, YANG K, CHI T, LIAO Z et al. PPAR-α modulators as current and potential cancer treatments. Front Oncol 2021; 11: 599995. https://doi.org/10.3389/fonc.2021.599995

[8] HERNANDEZ-QUILES M, BROEKEMA MF, KALKHOVEN E. PPARγ in metabolism, immunity, and cancer: Unified and diverse mechanisms of action. Front Endocrinol 2021; 12: 624112. https://doi.org/10.3389/fendo.2021.624112

[9] GRABACKA M, REISS K. Anticancer properties of PPARα—Effects on cellular metabolism and inflammation. PPAR Res 2008; 2008: 930705. https://doi.org/10.1155/2008/930705.

[10] AHMED W, ZIOUZENKOVA O, BROWN J, DEVCHAND P, FRANCIS S et al. PPARs and their metabolic modulation: New mechanisms for transcriptional regulation? J Intern Med 2007; 262: 184–198. https://doi.org/10.1111/j.1365-2796.2007.01825.x

[11] FINCK BN, KELLY DP. Peroxisome proliferator-activated receptor alpha (PPARα) signaling in the gene regulatory control of energy metabolism in the normal and diseased heart. J Mol Cell Cardiol 2002; 34: 1249–1257. https://doi.org/10.1006/jmcc.2002.2061

[12] LI Z, LUO L, YU W, LI P, OU D et al. PPARγ phase separates with RXRα at PPREs to regulate target gene expression. Cell Discov 2022; 8: 37. https://doi.org/10.1038/s41421-022-00388-0

[13] AMBER-VITOS O, CHATURVEDI N, NACHLIEL E, GUTMAN M, TSFADIA Y. The effect of regulating molecules on the structure of the PPAR-RXR complex. Biochim Biophys Acta 2016; 1861: 1852–1863. https://doi.org/10.1016/j.bbalip.2016.09.003

[14] BASILOTTA R, LANZA M, CASILI G, CHISARI G, MUNAO S et al. Potential therapeutic effects of PPAR ligands in glioblastoma. Cells 2002; 11: 621. https://doi.org/10.3390/cells11040621

[15] VITALE SG, LAGANA AS, NIGRO A, LA ROSA VL, ROSSETTI P, et al. Peroxisome proliferator-activated receptor modulation during metabolic diseases and cancers: Master and minions. PPAR Res 2016; 2016: 6517313. https://doi.org/10.1155/2016/6517313

[16] SPAGNOLO A, GRANT EN, GLICK R, LICHTOR T, FEINSTEIN DL. Differential effects of PPARγ agonists on the metabolic properties of gliomas and astrocytes. Neurosci Lett 2007; 417: 72–77. https://doi.org/10.1016/j.neulet.2007.02.036

[17] SHIGETO T, YOKOYAMA Y, XIN B, MIZUNUMA H. Peroxisome proliferator-activated receptor α and γ ligands inhibit the growth of human ovarian cancer. Oncol Rep 2007; 18: 833–840.

[18] DRUKALA K, URBANSKA A, WILK M, GRABACKA E, WYBIERALSKA L et al. ROS accumulation and IGF-IR inhibition contribute to fenofibrate/PPARα-mediated inhibition of glioma cell motility in vitro. Mol Cancer 2010; 9: 159. https://doi.org/10.1186/1476-4598-9-159

[19] MA Y, TEMKIN SM, HAWKRIDGE AM, GUO C, WANG W et al. Fatty acid oxidation: An emerging facet of metabolic transformation in cancer. Cancer Lett 2018; 435: 92–100. https://doi.org/10.1016/j.canlet.2018.08.006

[20] LAMICHANE S, DAHAL LAMICHANE B, KWON SM. Pivotal roles of peroxisome proliferator-activated receptors (PPARs) and their signal cascade for cellular and whole-body energy homeostasis. Int J Mol Sci 2018; 19: 949. https://doi.org/10.3390/ijms19040949

[21] ASGHARZADEH F, MEMARZIA A, ALIKHANI V, BEIGOLI S, BOSKABADY MH. Peroxisome proliferator-activated receptors: Key regulators of tumor progression and growth. Transl Oncol 2024; 47: 102039. https://doi.org/10.1016/j.tranon.2024.102039

[22] GOVINDARAJAN R, RATNASINGHE L, SIMMONS DL, SIEGEL ER, MIDATHADA MV et al. Thiazolidinediones and risk of lung, prostate, and colon cancer in patients with diabetes. J Clin Oncol 2007; 25: 1476–1481. https://doi.org/10.1200/JCO.2006.07.2777

[23] REDDY AT, LAKSHMI SP, REDDY RC. PPARγ as a novel therapeutic target in lung cancer. PPAR Res 2016; 2016: 8972570. https://doi.org/10.1155/2016/8972570

[24] CIARAMELLA V, SASSO FC, DI LIELLO R, CORTE CMD, BARRA G et al. Activity and molecular targets of pioglitazone via blockade of proliferation, invasiveness and bioenergetics in human NSCLC. J Exp Clin Cancer Res 2019; 38: 178. https://doi.org/10.1186/s13046-019-1176-1

[25] NANJAN MJ, MOHAMMED M, PRASHANTHA KUMAR BR, CHANDRASEKAR MJN. Thiazolidinediones as antidiabetic agents: A critical review. Bioorg Chem 2018; 77: 548–567. https://doi.org/10.1016/j.bioorg.2018.02.009

[26] SEE LC, WU CY, TSAI CY, LEE CC, CHEN JJ et al. PPAR-γ agonist pioglitazone and the risks of malignancy among type 2 diabetes mellitus patients. Acta Diabetol 2025; 62: 531–542. https://doi.org/10.1007/s00592-024-02378-y

[27] SKOCZYŃSKA A, OŁDAKOWSKA M, DOBOSZ A, ADAMIEC R, GRITSKEVICH S et al. PPARs in clinical experimental medicine after 35 years of worldwide scientific investigations and medical experiments. Biomolecules 2024; 14: 786. https://doi.org/10.3390/biom14070786

[28] WANG Q, GÜMÜŞ ZH, COLAROSSI C, MEMEO L, WANG X et al. SCLC: Epidemiology, risk factors, genetic susceptibility, molecular pathology, screening, and early detection. J Thorac Oncol 2023; 18: 31–46. https://doi.org/10.1016/j.jtho.2022.10.002

[29] HAMILTON G, BURGHUBER O, ZEILLINGER R. Circulating tumor cells in small cell lung cancer: Ex vivo expansion. Lung 2015; 193: 451–452. https://doi.org/10.1007/s00408-015-9725-7

[30] KLAMETH L, RATH B, HOCHMAIER M, MOSER D, REDL M et al. Small cell lung cancer: Model of circulating tumor cell tumorospheres in chemoresistance. Sci Rep 2017; 7: 5337. https://doi.org/10.1038/s41598-017-05562-z

[31] SHIMADA Y, SUDO T, AKAMATSU S, SUNADA T, MYOMOTO A et al. Cell lines of circulating tumor cells: What is known and what needs to be resolved. J Pers Med 2022; 12: 666. https://doi.org/10.3390/jpm12050666

[32] DEBERARDINIS RJ, CHANDEL NS. Fundamentals of cancer metabolism. Sci Adv 2016; 2: e1600200. https://doi.org/10.1126/sciadv.1600200

[33] MA Y, WANG B, LI L, WANG F, XIA X. The administration of peroxisome proliferator-activated receptors α/γ agonist TZD18 inhibits cell growth and induces apoptosis in human gastric cancer cell lines. J Cancer Res Ther 2019; 15: 120–125. https://doi.org/10.4103/0973-1482.208753

[34] WAGNER N, WAGNER KD. Peroxisome proliferator-activated receptors and the hallmarks of cancer. Cells 2022; 11: 2432. https://doi.org/10.3390/cells11152432

[35] LEHMANN JM, MOORE LB, SMITH-OLIVER TA, WILKISON WO, WILLSON TM et al. An antidiabetic thiazolidinedione is a high affinity ligand for peroxisome proliferator-activated receptor gamma (PPARγ). J Biol Chem 1995; 270: 12953–12956. https://doi.org/10.1074/jbc.270.22.12953

[36] SHANG J, KOJETIN DJ. Structural mechanism underlying ligand binding and activation of PPARγ. Structure 2021; 29: 940–950.e4. https://doi.org/10.1016/j.str.2021.02.006

[37] LEESNITZER LM, PARKS DJ, BLEDSOE RK, COBB JE, COLLINS JL et al. Functional consequences of cysteine modification in the ligand binding sites of peroxisome proliferator activated receptors by GW9662. Biochemistry 2002; 41: 6640–6650. https://doi.org/10.1021/bi0159581

[38] OLIVER WR JR, SHENK JL, SNAITH MR, RUSSELL CS, PLUNKET KD et al. A selective peroxisome proliferator-activated receptor delta agonist promotes reverse cholesterol transport. Proc Natl Acad Sci U S A 2001; 98: 5306–5311. https://doi.org/10.1073/pnas.091021198

[39] PHAN ANH, VO VTA, HUA TNM, KIM MK, JO SY et al. PPARγ sumoylation-mediated lipid accumulation in lung cancer. Oncotarget 2017; 8: 82491–82505. https://doi.org/10.18632/oncotarget.19700

[40] ANDELA VB, ALTUWAIJRI S, WOOD J, ROSIER RN. Inhibition of beta-oxidative respiration is a therapeutic window associated with the cancer chemo-preventive activity of PPARγ agonists. FEBS Lett 2005; 579: 1765–1769. https://doi.org/10.1016/j.febslet.2005.01.082

[41] URBANSKA K, PANNIZZO P, GRABACKA M, CROUL S, DEL VALLE L et al. Activation of PPARα inhibits IGF-I-mediated growth and survival responses in medulloblastoma cell lines. Int J Cancer 2008; 123: 1015–1024. https://doi.org/10.1002/ijc.23588

[42] CHI T, WANG M, WANG X, YANG K, XIE F et al. PPAR-γ modulators as current and potential cancer treatments. Front Oncol 2021; 11: 737776. https://doi.org/10.3389/fonc.2021.737776

[43] AHMADIAN M, SUH JM, HAH N, LIDDLE C, ATKINS AR et al. PPARγ signaling and metabolism: The good, the bad and the future. Nat Med 2013; 19: 557–566. https://doi.org/10.1038/nm.3159

[44] ZHANG J, TANG M, SHANG J. PPARγ modulators in lung cancer: Molecular mechanisms, clinical prospects, and challenges. Biomolecules 2024; 14: 190. https://doi.org/10.3390/biom14020190

[45] GRAU R, PUNZÓN C, FRESNO M, IÑIGUEZ MA. Peroxisome-proliferator-activated receptor alpha agonists inhibit cyclo-oxygenase-2 and vascular endothelial growth factor transcriptional activation in human colorectal carcinoma cells via inhibition of activator protein-1. Biochem J 2006; 395: 81–88. https://doi.org/10.1042/BJ20050964

[46] MEISSNER M, BERLINSKI B, GILLE J, DOLL M, KAUFMANN R. Peroxisome proliferator-activated receptor-α agonists suppress transforming growth factor-α-induced matrix metalloproteinase-9 expression in human keratinocytes. Clin Exp Dermatol 2011; 36: 911–914. https://doi.org/10.1111/j.1365-2230.2011.04125.x

[47] NINOMIYA I, YAMAZAKI K, OYAMA K, HAYASHI H, TAJIMA H et al. Pioglitazone inhibits the proliferation and metastasis of human pancreatic cancer cells. Oncol Lett 2014; 8: 2709–2714. https://doi.org/10.3892/ol.2014.2553

[48] RATH B, PLANGGER A, KRENBEK D, HOCHMAIR M, STICKLER S et al. Rovalpituzumab tesirine resistance: Analysis of a corresponding small cell lung cancer and circulating tumor cell line pair. Anticancer Drugs 2022; 33: 300–307. https://doi.org/10.1097/CAD.0000000000001267

[49] SABRI N. Determination of pioglitazone hydrochloride in human plasma by high performance liquid chromatography and its pharmacokinetics application. CATRINA 2009; 4: 45–52.

[50] XIU MX, LIU YM, KUANG BH. The role of DLLs in cancer: A novel therapeutic target. Onco Targets Ther 2020; 13: 3881–3901. https://doi.org/10.2147/OTT.S244860
[51] SEARGENT JM, YATES EA, GILL JH. GW9662, a potent antagonist of PPARγ, inhibits growth of breast tumour cells and promotes the anticancer effects of the PPARγ agonist rosiglitazone, independently of PPARγ activation. Br J Pharmacol 2004; 143: 933–937. https://doi.org/10.1038/sj.bjp.0705973
[52] IM CN. Combination treatment with PPARγ ligand and its specific inhibitor GW9662 downregulates BIS and 14-3-3 gamma, inhibiting stem-like properties in glioblastoma cells. Biomed Res Int 2017; 2017: 5832824. https://doi.org/10.1155/2017/5832824
[53] DENG G, LIU Z, YE F, LUO X, ZHU W, et al. Tryptophan-containing dipeptide derivatives as potent PPARγ antagonists: Design, synthesis, biological evaluation, and molecular modeling. Eur J Med Chem 2008; 43: 2699–2716. https://doi.org/10.1016/j.ejmech.2008.01.032
[54] CASTELLI V, CATANESI M, ALFONSETTI M, LAEZZA C, LOMBARDI F et al. PPARα-selective antagonist GW6471 inhibits cell growth in breast cancer stem cells inducing energy imbalance and metabolic stress. Biomedicines 2021; 9: 127. https://doi.org/10.3390/biomedicines9020127
[55] JANG HY, HONG OY, YOUN HJ, JUNG J, CHUNG EY et al. CDDO, a PPAR-γ ligand, inhibits TPA-induced cell migration and invasion through a PPAR-γ-independent mechanism. Oncol Lett 2022; 24: 354. https://doi.org/10.3892/ol.2022.13474
[56] GE LN, YAN L, LI C, CHENG K. Bavachinin exhibits antitumor activity against non-small cell lung cancer by targeting PPARγ. Mol Med Rep 2019; 20: 2805–2811. https://doi.org/10.3892/mmr.2019.10485
[57] YUE H, TIAN Y, ZHAO Z, BO Y, GUO Y et al. Comparative study of docosahexaenoic acid with different molecular forms for promoting apoptosis of the 95D non-small-cell lung cancer cells in a PPARγ-dependent manner. Mar Drugs 2022; 20: 599. https://doi.org/10.3390/md20100599
[58] HAN S, ROMAN J. Rosiglitazone suppresses human lung carcinoma cell growth through PPARγ-dependent and PPARγ-independent signal pathways. Mol Cancer Ther 2006; 5: 430–437. https://doi.org/10.1158/1535-7163.MCT-05-0347
[59] KIM KY, AHN JH, CHEON HG. Apoptotic action of peroxisome proliferator-activated receptor-gamma activation in human non-small-cell lung cancer is mediated via proline oxidase-induced reactive oxygen species formation. Mol Pharmacol 2007; 72: 674–685. https://doi.org/10.1124/mol.107.035584
[60] YIN H, LIU Y, YUE H, TIAN Y, DONG P et al. DHA- and EPA-enriched phosphatidylcholine suppress human lung carcinoma 95D cells metastasis via activating the peroxisome proliferator-activated receptor γ. Nutrients 2022; 14: 4675. https://doi.org/10.3390/nu14214675
[61] CHOUDHARY R, LI H, WINN RA, SORENSON AL, WEISER-EVANS MC et al. Peroxisome proliferator-activated receptor-gamma inhibits transformed growth of non-small cell lung cancer cells through selective suppression of Snail. Neoplasia 2010; 12: 224–234. https://doi.org/10.1593/neo.91638
[62] YOSHIZUMI T, OHTA T, NINOMIYA I, TERADA I, FUSHIDA S et al. Thiazolidinedione, a peroxisome proliferator-activated receptor-gamma ligand, inhibits growth and metastasis of HT-29 human colon cancer cells through differentiation-promoting effects. Int J Oncol 2004; 25: 631–639.
[63] PANIGRAHY D, SINGER S, SHEN LQ, BUTTERFIELD CE, FREEDMAN DA et al. PPARγ ligands inhibit primary tumor growth and metastasis by inhibiting angiogenesis. J Clin Invest 2002; 110: 923–932. https://doi.org/10.1172/JCI15634
[64] TAKANO S, KUBOTA T, NISHIBORI H, HASEGAWA H, ISHII Y et al. Pioglitazone, a ligand for peroxisome proliferator-activated receptor-gamma, acts as an inhibitor of colon cancer liver metastasis. Anticancer Res 2008; 28: 3593–3599.
[65] JANG JH, LEE TJ, SUNG EG, SONG IH, KIM JY. Pioglitazone mediates apoptosis in Caki cells via downregulating c-FLIP(L) expression and reducing Bcl-2 protein stability. Oncol Lett 2021; 22: 743. https://doi.org/10.3892/ol.2021.13004
[66] MENENDEZ-GUTIERREZ MP, ROSZER T, RICOTE M. Biology and therapeutic applications of peroxisome proliferator-activated receptors. Curr Top Med Chem 2012; 12: 548–584. https://doi.org/10.2174/156802612799436669
[67] TSUBAKI M, TAKEDA T, TOMONARI Y, KAWASHIMA K, ITOH T et al. Pioglitazone inhibits cancer cell growth through STAT3 inhibition and enhanced AIF expression via a PPARγ-independent pathway. J Cell Physiol 2018; 233: 3638–3647. https://doi.org/10.1002/jcp.26225
[68] JIAO XX, LIN SY, LIAN SX, QIU YR, LI ZH et al. The inhibition of the breast cancer by PPARγ agonist pioglitazone through JAK2/STAT3 pathway. Neoplasma 2020; 67: 834–842. https://doi.org/10.4149/neo_2020_190805N716
[69] WANG Z, SHEN W, LI X, FENG Y, QIAN K et al. The PPARγ agonist rosiglitazone enhances the radiosensitivity of human pancreatic cancer cells. Drug Des Devel Ther 2020; 14: 3099–3110. https://doi.org/10.2147/DDDT.S242557
[70] ZHANG W, SHAO W, DONG Z, ZHANG S, LIU C et al. Cloxiquine, a traditional antituberculosis agent, suppresses the growth and metastasis of melanoma cells through activation of PPARγ. Cell Death Dis 2019; 10: 404. https://doi.org/10.1038/s41419-019-1644-8
[71] WANG S, ZHANG Q, ZHANG Y, SHEN C, WANG Z et al. Agrimol B suppresses adipogenesis through modulation of SIRT1–PPARγ signal pathway. Biochem Biophys Res Commun 2016; 477: 454–460. https://doi.org/10.1016/j.bbrc.2016.06.078[72] LIAN X, WANG G, ZHOU H, ZHENG Z, FU Y et al. Anticancer properties of fenofibrate: A repurposing use. J Cancer 2018; 9: 1527–1537. https://doi.org/10.7150/jca.24488
[73] CHEN YC, CHEN JH, TSAI CF, WU CT, CHANG PC et al. Inhibition of tumor migration and invasion by fenofibrate via suppressing epithelial–mesenchymal transition in breast cancers. Toxicol Appl Pharmacol 2024; 483: 116818. https://doi.org/10.1016/j.taap.2024.116818
[74] ADHIKARY T, BRANDT DT, KADDATZ K, STOCKERT J, NARUHN S et al. Inverse PPARβ/δ agonists suppress oncogenic signaling to the ANGPTL4 gene and inhibit cancer cell invasion. Oncogene 2013; 32: 5241–5252. https://doi.org/10.1038/onc.2012.549

[75] LEITER A, CHAROKOPOS A, BAILEY S, GALLAGHER EJ, HIRSCH FR et al. Assessing the association of diabetes with lung cancer risk. Transl Lung Cancer Res 2021; 10: 4200–4208. https://doi.org/10.21037/tlcr-21-601

[76] HATLEN P, GRØNBERG BH, LANGHAMMER A, CARLSEN SM, AMUNDSEN T. Prolonged survival in patients with lung cancer with diabetes mellitus. J Thorac Oncol 2011; 6: 1810–1817. https://doi.org/10.1097/JTO.0b013e31822a75be

[77] HO YS, YIP LY, BASRI N, CHONG VS, TEO CC et al. Lipidomic profiling of lung pleural effusion identifies unique metabotype for EGFR mutants in non-small cell lung cancer. Sci Rep 2016; 6: 35110. https://doi.org/10.1038/srep35110

[78] YANG Z, SONG Z, CHEN Z, GUO Z, JIN H et al. Metabolic and lipidomic characterization of malignant pleural effusion in human lung cancer. J Pharm Biomed Anal 2020; 180: 113069. https://doi.org/10.1016/j.jpba.2019.113069

[79] HAMILTON G, RATH B, STICKLER S. Significance of circulating tumor cells in lung cancer: A narrative review. Transl Lung Cancer Res 2023; 12: 877–894. https://doi.org/10.21037/tlcr-22-712

[80] HAMILTON G, HOCHMAIR MJ, STICKLER S. Overcoming resistance in small-cell lung cancer. Expert Rev Respir Med 2024; 18: 569–580. https://doi.org/10.1080/17476348.2024.2388288

https://doi.org/10.4149/neo_2025_250917N396

Peroxisome proliferator-activated receptors as novel targets of small cell lung cancer circulating tumor cells

Gerhard HAMILTON[1,*], Marie-Therese EGGERSTORFER[1], Lukas WEIGL[2], Maximilian Johannes HOCHMAIR[3], Sandra STICKLER[1]

Supplementary Information

Supplementary Table S1. RNA-sequencing data (Illumina. both directions). with gene expression values normalized to transcripts per million (TPM). of CTC-derived BHGc16 and BHGc10. as well as pleural effusion-derived S457 and S1392.

	BHGc16	BHGc10	S457	S1392
ASCL1	562	920	313.6	1
YAP1	0.89	0.1	0.09	1.5
NEURO D1	2.9	0.74	1.8	4.1
POUF3	0.16	0	0.01	540
CHGA	322	274	493.3	22.4
SYP	99.4	95.3	126	69.6
ENO1	778	605	1009.5	113
RB1	7.2	19	5.6	43.4

Supplementary Table S2. PPAR-directed compounds of the Transcription Factor Library L1380 (Batch #PHD156583, Targetmol, Welesely Hills, MA, USA) and their IC50-values derived from dose-response curves.

Compound	ID	Mechanism	BHGc16	BHGc10
			IC50 [μM]	
GW9662	T2260	PPARγ antagonist	4.29	18.57
Clofibrate	T1298	PPARα agonist	>20	>20
Pioglitazone	T0214	PPARγ agonist	1.65	5.89
Rosiglitazone	T0334	PPARγ agonist	>20	>20
Cloxiquine	T0509	PPARα agonist	4.29	5.9
Pioglitazone hydrochloride	T0214L	PPARγ agonist (salt)	>20	>20
Retinoic acid	T1051	TargetMol annotation (PPAR assigned; putative modulator, in silico/screening evidence)	>20	>20
Repaglinide	T1088	TargetMol annotation (PPAR assigned; putative modulator, in silico/screening evidence)	>20	>20
Fenofibrate	T1149	PPARα agonist	2.19	19.64
Ciprofibrate	T1264	PPARα agonist	>20	>20
5-Aminosalicylic Acid	T0646	PPARγ agonist (weak/putative)	>20	>20
Triflusal	T0705	TargetMol annotation (PPAR assigned; putative modulator, in silico/screening evidence)	>20	>20
Bezafibrate	T0841	Pan-PPAR agonist (α/δ/γ)	15.71	>20
Fenofibric acid	T1402	PPARα agonist	>20	>20
Gemfibrozil	T1415	PPARα agonist	>20	>20
Nateglinide	T1674	TargetMol annotation (PPAR assigned; putative modulator, in silico/screening evidence)	>20	>20
Rosiglitazone maleate	T1622	PPARγ agonist (salt)	3.13	>20
carbidopa monohydrate	T2269	TargetMol annotation (PPAR assigned; putative modulator, in silico/screening evidence)	>20	>20
Bavachinin	T3056	PPARγ agonist (reported)	14.29	14.28
Icariin	T2855	PPARγ agonist (reported)	>20	>20
Gypenoside XLIX	T2985	PPARγ agonist (reported)	>20	>20
Astaxanthin	T3138	PPARα agonist / PPARγ antagonist (reported)	>20	>20
Ginsenoside Rh1	T2932	PPARγ agonist (reported)	>20	>20
Ramatroban	T2396	TargetMol annotation (PPAR assigned; putative modulator, in silico/screening evidence)	>20	>20
GSK3787	T1941	PPARδ antagonist	18.21	>20
Troglitazone	T3170	PPARγ agonist	20	>20
PHYTOL	T3254	PPARα agonist (via phytanic acid pathway)	18.2	>20

Supplementary Table S2. ***Continued . . .***

Compound	ID	Mechanism	BHGc16	BHGc10
			IC50 [μM]	
Eupatilin	T3362	PPARα activator (reported)	>20	>20
T0070907	T6689	PPARγ antagonist	4.02	14.29
Glabridin	T3403	PPARγ agonist (reported)	13.21	11.79
GW 501516	T6151	PPARδ agonist	>20	>20
XMD8-87	T3709	TargetMol annotation (PPAR assigned; putative modulator, in silico/screening evidence)	>20	12.86
XMD16-5	T3710	TargetMol annotation (PPAR assigned; putative modulator, in silico/screening evidence)	>20	>20
MK-886	T6893	PPARα antagonist (also FLAP inhibitor)	9.64	10
Alpinetin	T3867	PPARγ agonist (reported)	17.14	>20
Choline Fenofibrate	T3941	PPARα agonist (prodrug)	>20	>20
Adelmidrol	T3954	PPARα modulator (PEA analog; reported)	>20	>20
Palmitoylethanolamide	T6926	PPARα agonist	>20	>20
Cinnamyl alcohol	T5S1550	TargetMol annotation (PPAR assigned; putative modulator, in silico/screening evidence)	>20	>20
Raspberry ketone	T2S0633	PPARα activator (reported)	>20	>20
Bilobetin	T4S2128	PPARα agonist (supports α-mediated lipid catabolism)	7.1	6.18
Protopanaxatriol	T3917	PPARγ agonist (reported)	10.94	15.2
GW0742	T6524	PPARδ agonist	>20	>20
Elafibranor	T4408	PPARα/δ agonist	8.99	15.15
Seladelpar	T4628	PPARδ agonist	>20	9.48
BMS-687453	T5532	PPARγ partial agonist	>20	>20
Alliin	T5764	PPARγ activator (reported)	>20	>20
Rosiglitazone hydrochloride	T6646	PPARγ agonist (salt)	>20	>20
DG172 dihydrochloride	T7821	PPARδ antagonist (putative)	7.86	13.52
SC-236	T8505	TargetMol annotation (PPAR assigned; putative modulator, in silico/screening evidence)	18	>20
Sakuranetin	TN1126	PPARγ agonist (reported)	>20	>20
GW1929	TQ0156	PPARγ agonist	>20	>20
GW7647	T15453	PPARα agonist	13.82	13.16
GW6471	T8486	PPARα antagonist	4.4	7.74
Oleoylethanolamide	T12296	PPARα agonist	>20	>20
AMG131	T8780	TargetMol annotation (PPAR assigned; putative modulator, in silico/screening evidence)	18.58	>20
Arhalofenate	T16022	PPARγ partial agonist / modulator	>20	>20
Pemafibrate	TQ0107	PPARα agonist (SPPARMα)	13.16	>20
LJ570	T8374	TargetMol annotation (PPAR assigned; putative modulator, in silico/screening evidence)	>20	>20
NTP42	T12268	TargetMol annotation (PPAR assigned; putative modulator, in silico/screening evidence)	>20	>20
LY518674	T15821	PPARα agonist (SPPARMα)	>20	>20
Lonazolac	T50025	PPARγ weak agonist (NSAID class)	>20	>20
GFT505	T8699	PPARα/δ agonist	4.82	5.94
SR 16832	T24827	PPARγ antagonist	4.93	1.76
Bocidelpar	T39516	PPARδ agonist	>20	>20
Tetradecylthioacetic acid	T9808	PPARα agonist (reported pan-PPAR)	>20	>20
N-Oleoyl glycine	T13803	PPARα agonist (reported)	>20	>20
Darglitazone	T22708	PPARγ agonist	>20	11.61
Furegrelate	T11339L	TargetMol annotation (PPAR assigned; putative modulator, in silico/screening evidence)	>20	>20
Furegrelate sodium	T11339	TargetMol annotation (PPAR assigned; putative modulator, in silico/screening evidence)	>20	>20
GW590735	T9766	PPARδ agonist (reported)	>20	>20
CC618	T9767	PPARβ/δ antagonist (covalent)	3.04	>20
MCC-555	T21764	PPARγ agonist	>20	>20
beta-Amyrone	TN3500	TargetMol annotation (PPAR assigned; putative modulator, in silico/screening evidence)	13.82	>20
Inolitazone	T15581	PPARγ agonist	>20	17.51
GQ-16	T21955	PPARγ partial agonist	>20	17.52
Magnolol	T3000	PPARγ agonist	>20	>20
EPI-001	T6829	TargetMol annotation (PPAR assigned; putative modulator, in silico/screening evidence)	>20	18.76

Supplementary Table S2. ***Continued . . .***

Compound	ID	Mechanism	BHGc16	BHGc10
			IC50 [μM]	
Mifobate	T16074	TargetMol annotation (PPAR assigned; putative modulator, in silico/screening evidence)	>20	>20
FH535	T2413	PPARδ/γ antagonist	>20	>20
Abietic Acid	T3090	PPARα/γ dual agonist (reported)	>20	>20
Glipizide	T1603	TargetMol annotation (PPAR assigned; putative modulator, in silico/screening evidence)	>20	15.62
Oroxin A	T5S0788	PPARγ agonist (reported)	>20	>20
Fisetin	T2879	PPARγ activator (reported)	>20	>20
Agrimol B	T4S1173	PPARγ pathway modulator	3.87	2.45
RGX-202	T7535	TargetMol annotation (PPAR assigned; putative modulator, in silico/screening evidence)	>20	>20
Fucosterol	T8184	PPARα agonist (reported)	1.08	>20
Kudinoside D	TN1836	TargetMol annotation (PPAR assigned; putative modulator, in silico/screening evidence)	>20	>20
Norathyriol	TN1990	TargetMol annotation (PPAR assigned; putative modulator, in silico/screening evidence)	17	15
EHP-101	T13289	TargetMol annotation (PPAR assigned; putative modulator, in silico/screening evidence)	>20	>20
Palmitelaidic Acid	T19500	PPARα/γ weak endogenous ligand (fatty acid)	>20	>20
CDDO-Im	TQ0120	PPARγ partial agonist / modulator	<0.16	<0.16
Tetramethylkaempferol	TN5137	PPARγ agonist (reported)	>20	>20
Uvaol	TN2290	PPARα/γ dual activator (reported)	>20	>20
MA-0204	T15945	PPARδ modulator / agonist (highly selective)	1.15	>20
SR1664	T23389	PPARγ non-agonist antagonist (blocks Cdk5-mediated Ser273 phosphorylation)	<0.16	>20

Note: Standard deviation is below 6.1% of the IC50-mean values

Supplementary Table S3. PPAR-directed compounds of the Transcription Factor Library L1380 (Batch # PHD156583, Targetmol, Welesely Hills, MA, USA) with IC50-values below 9 μM, as derived from dose-response curves.

Compound	ID	Mechanism	BHGc16	BHGc10	NCI-H69	S457	S1392
			IC50 [μM]				
GW9662	T2260	PPARγ antagonist	4.29	18.57	7.9	6.92	6.74
T0070907	T6689	PPARγ antagonist	4.02	14.29	9.11	8.15	7.31
Bilobetin	T4S2128	PPARα agonist (supports α-mediated lipid catabolism)	7.1	6.18	>20	6.02	>20
GW6471	T8486	PPARα antagonist	4.4	7.74	8.38	8.77	>20
MA-0204	T15945	PPARβ/δ modulator / agonist (highly selective)	1.15	>20	>20	>20	>20
GFT505	T8699	PPARα/δ agonist	4.82	5.94	7.94	5.34	>20
SR1664	T23389	PPARγ non-agonist antagonist (blocks Cdk5-mediated Ser273 phosphorylation)	<0.16	>20	>20	>20	>20
SR 16832	T24827	PPARγ antagonist	4.93	1.76	0.18	0.26	0.61
CC618	T9767	PPARβ/δ antagonist	3.04	>20	0.28	nd	>20
Fucosterol	T8184	PPARα agonist	1.08	>20	2.44	3.89	5
CDDO-Im	TQ0120	PPARγ partial agonist / modulator	<0.16	<0.16	0.26	0.99	<0.16

Standard deviation is below 4.7% of the IC50-mean values

Supplement A

BCL-x

ANOVA result: F = 436.4834, p = 0.03045

Descriptive Statistics

Treatment Group	Mean	Standard Error (SE)	95% CI Lower	95% CI Upper
BHG16 Control	388.86	3.23148	347.80018	429.91982
Pioglitazone	410.79	0.36062	406.20783	415.37217
Rosiglitazone	438.88	4.03758	387.57769	490.18231
Cloxiquine	120.14	1.87383	96.33069	143.94931

Tukey Grouping

Treatment Group	Tukey Group
Control	A
Rosiglitazone	B
Pioglitazone	C
Cloxiquine	D

Pairwise Comparisons

Comparison	Mean Difference	Std. Error	p-value	95.00% LCL	95.00% UCL
Control vs Pioglitazone	-21.93	2.28132	0.00726	-32.9391	-10.9209
Control vs Rosiglitazone	-50.02	2.28132	6.36288E-4	-61.0291	-39.0109
Control vs Cloxiquine	268.72	2.28132	<0.0001	257.7109	279.7291
Pioglitazone vs Rosiglitazone	-28.09	2.28132	0.00352	-39.0991	-17.0809
Pioglitazone vs Cloxiquine	290.65	2.28132	<0.0001	279.6409	301.6591
Rosiglitazone vs Cloxiquine	318.74	2.28132	<0.0001	307.7309	329.7491

CapG

ANOVA result: F = 158.54994, p = 0.05045

Descriptive Statistics

Treatment Group	Mean	Standard Error (SE)	95% CI Lower	95% CI Upper

BHG16 Control	123.14	29.23179	-248.28516	494.56516
Pioglitazone	185.37	14.60883	-0.25274	370.99274
Rosiglitazone	231.81	7.7711	133.06877	330.55123
Cloxiquine	137.96	2.25567	109.29899	166.62101

Pairwise Comparisons

Comparison	Mean Difference	Std. Error	p-value	95.00% LCL	95.00% UCL
Control vs Pioglitazone	-62.23	16.49181	0.09382	-141.81567	17.35567
Control vs Rosiglitazone	-108.67	16.49181	0.02136	-188.25567	-29.08433
Control vs Cloxiquine	-14.82	16.49181	0.80861	-94.40567	64.76567
Pioglitazone vs Rosiglitazone	-46.44	16.49181	0.18441	-126.02567	33.14567
Pioglitazone vs Cloxiquine	47.41	16.49181	0.17638	-32.17567	126.99567
Rosiglitazone vs Cloxiquine	93.85	16.49181	0.03207	14.26433	173.43567

Cathepsin S

ANOVA result: F = 7672.11839, p = 0.00727

Descriptive Statistics

Treatment Group	Mean	Standard Error (SE)	95% CI Lower	95% CI Upper
BHG16 Control	274.31	5.14774	208.9018	339.7182
Pioglitazone	274.28	1.37886	256.75995	291.80005
Rosiglitazone	321.87	0.34648	317.46752	326.27248
Cloxiquine	163.87	4.93561	101.15719	226.58281

Pairwise Comparisons

Comparison	Mean Difference	Std. Error	p-value	95.00% LCL	95.00% UCL
Control vs Pioglitazone	0.03	3.46597	1	-16.69599	16.75599
Control vs Rosiglitazone	-47.56	3.46597	0.00256	-64.28599	-30.83401
Control vs Cloxiquine	110.44	3.46597	2.08232E-4	93.71401	127.16599
Pioglitazone vs Rosiglitazone	-47.59	3.46597	0.00255	-64.31599	-30.86401

Pioglitazone vs Cloxiquine	110.41	3.46597	2.08401E-4	93.68401	127.13599
Rosiglitazone vs Cloxiquine	158	3.46597	7.11544E-5	141.27401	174.72599

DLL1

ANOVA result: F = 863.10232, p = 0.02166

Descriptive Statistics

Treatment Group	Mean	Standard Error (SE)	95% CI Lower	95% CI Upper
BHG16 Control	474.38	4.61741	415.71028	533.04972
Pioglitazone	489.69	20.79601	225.45163	753.92837
Rosiglitazone	549.2	29.13987	178.94284	919.45716
Cloxiquine	127.03	1.27986	110.7678	143.2922

Pairwise Comparisons

Comparison	Mean Difference	Std. Error	p-value	95.00% LCL	95.00% UCL
Control vs Pioglitazone	-15.31	18.71237	0.84395	-105.6116	74.9916
Control vs Rosiglitazone	-74.82	18.71237	0.08124	-165.1216	15.4816
Control vs Cloxiquine	347.35	18.71237	0.00104	257.0484	437.6516
Pioglitazone vs Rosiglitazone	-59.51	18.71237	0.14084	-149.8116	30.7916
Pioglitazone vs Cloxiquine	362.66	18.71237	9.18964E-4	272.3584	452.9616
Rosiglitazone vs Cloxiquine	422.17	18.71237	5.84347E-4	331.8684	512.4716

Enolase 2

ANOVA result: F = 1202.61624, p = 0.01835

Descriptive Statistics

Treatment Group	Mean	Standard Error (SE)	95% CI Lower	95% CI Upper
BHG16 Control	698.6	25.88718	369.6722	1027.5278
Pioglitazone	344.16	18.11608	113.97343	574.34657
Rosiglitazone	518.89	2.19203	491.03761	546.74239
Cloxiquine	647.99	17.52211	425.35053	870.62947

Pairwise Comparisons

Comparison	Mean Difference	Std. Error	p-value	95.00% LCL	95.00% UCL
Control vs Pioglitazone	354.44	14.02833	4.16745E-4	286.74253	422.13747
Control vs Rosiglitazone	179.71	14.02833	0.00313	112.01253	247.40747
Control vs Cloxiquine	50.61	14.02833	0.10467	-17.08747	118.30747
Pioglitazone vs Rosiglitazone	-174.73	14.02833	0.0034	-242.42747	-107.03253
Pioglitazone vs Cloxiquine	-303.83	14.02833	6.60018E-4	-371.52747	-236.13253
Rosiglitazone vs Cloxiquine	-129.1	14.02833	0.00824	-196.79747	-61.40253

EpCAM/TROP1

ANOVA result: F = 204.28814, p = 0.04447

Descriptive Statistics

Treatment Group	Mean	Standard Error (SE)	95% CI Lower	95% CI Upper
BHG16 Control	410.7	4.23557	356.88199	464.51801
Pioglitazone	342.44	48.74087	-276.87148	961.75148
Rosiglitazone	169.74	34.93815	-274.19124	613.67124
Cloxiquine	349.04	1.0748	335.38334	362.69666

Pairwise Comparisons

Comparison	Mean Difference	Std. Error	p-value	95.00% LCL	95.00% UCL
Control vs Pioglitazone	68.26	33.02185	0.3347	-91.09584	227.61584
Control vs Rosiglitazone	240.96	33.02185	0.01602	81.60416	400.31584
Control vs Cloxiquine	61.66	33.02185	0.3946	-97.69584	221.01584
Pioglitazone vs Rosiglitazone	172.7	33.02185	0.04033	13.34416	332.05584
Pioglitazone vs Cloxiquine	-6.6	33.02185	0.99658	-165.95584	152.75584
Rosiglitazone vs Cloxiquine	-179.3	33.02185	0.03644	-338.65584	-19.94416

ErbB3/Her3

ANOVA result: F = 514.21233, p =0.02806

Descriptive Statistics

Treatment Group	Mean	Standard Error (SE)	95% CI Lower	95% CI Upper
BHG16 Control	216.36	10.15405	87.34052	345.37948
Pioglitazone	142.66	2.51023	110.76452	174.55548
Rosiglitazone	116.74	12.24002	-38.78418	272.26418
Cloxiquine	104.69	0.69296	95.88505	113.49495

Pairwise Comparisons

Comparison	Mean Difference	Std. Error	p-value	95.00% LCL	95.00% UCL
Control vs Pioglitazone	73.7	7.9958	0.0082	35.1141	112.2859
Control vs Rosiglitazone	99.62	7.9958	0.0034	61.0341	138.2059
Control vs Cloxiquine	111.67	7.9958	0.00243	73.0841	150.2559
Pioglitazone vs Rosiglitazone	25.92	7.9958	0.13479	-12.6659	64.5059
Pioglitazone vs Cloxiquine	37.97	7.9958	0.05217	-0.6159	76.5559
Rosiglitazone vs Cloxiquine	12.05	7.9958	0.52873	-26.5359	50.6359

p27/Kip1

ANOVA result: F = 418.46597, p = 0.0311

Descriptive Statistics

Treatment Group	Mean	Standard Error (SE)	95% CI Lower	95% CI Upper
BHG16 Control	145	3.97394	94.5063	195.4937
Pioglitazone	70.42	12.39558	-87.0808	227.9208
Rosiglitazone	146.15	6.25082	66.72575	225.57425
Cloxiquine	110.13	0.43841	104.55952	115.70048

Pairwise Comparisons

Comparison	Mean Difference	Std. Error	p-value	95.00% LCL	95.00% UCL
Control vs Pioglitazone	74.58	7.1078	0.00563	40.27942	108.88058

Control vs Rosiglitazone	-1.15	7.1078	0.99817	-35.45058	33.15058
Control vs Cloxiquine	34.87	7.1078	0.04786	0.56942	69.17058
Pioglitazone vs Rosiglitazone	-75.73	7.1078	0.00538	-110.03058	-41.42942
Pioglitazone vs Cloxiquine	-39.71	7.1078	0.03372	-74.01058	-5.40942
Rosiglitazone vs Cloxiquine	36.02	7.1078	0.04389	1.71942	70.32058

Serpin B5/Maspin

ANOVA result: F = 8910.2449, p =0.00674

Descriptive Statistics

Treatment Group	Mean	Standard Error (SE)	95% CI Lower	95% CI Upper
BHG16 Control	588.01	0.70711	579.02536	596.99464
Pioglitazone	513.8	10.79045	376.69434	650.90566
Rosiglitazone	518.54	2.53851	486.28513	550.79487
Cloxiquine	303.29	6.34275	222.69775	383.88225

Pairwise Comparisons

Comparison	Mean Difference	Std. Error	p-value	95.00% LCL	95.00% UCL
Control vs Pioglitazone	74.21	6.31317	0.00403	43.74408	104.67592
Control vs Rosiglitazone	69.47	6.31317	0.0049	39.00408	99.93592
Control vs Cloxiquine	284.72	6.31317	7.34857E-5	254.25408	315.18592
Pioglitazone vs Rosiglitazone	-4.74	6.31317	0.87174	-35.20592	25.72592
Pioglitazone vs Cloxiquine	210.51	6.31317	1.81756E-4	180.04408	240.97592
Rosiglitazone vs Cloxiquine	215.25	6.31317	1.7003E-4	184.78408	245.71592

Survivin

ANOVA result: F = 1935.93608, p = 0.01447

Descriptive Statistics

Treatment Group	Mean	Standard Error (SE)	95% CI Lower	95% CI Upper

BHG16 Control	770.48	20.87379	505.25332	1035.70668
Pioglitazone	698.9	11.10158	557.8411	839.9589
Rosiglitazone	742.3	13.06026	576.35363	908.24637
Cloxiquine	267.65	11.31371	123.8957	411.4043

Pairwise Comparisons

Comparison	Mean Difference	Std. Error	p-value	95.00% LCL	95.00% UCL
Control vs Pioglitazone	71.58	6.5176	0.00492	40.12757	103.03243
Control vs Rosiglitazone	28.18	6.5176	0.0666	-3.27243	59.63243
Control vs Cloxiquine	502.83	6.5176	1.25433E-5	471.37757	534.28243
Pioglitazone vs Rosiglitazone	-43.4	6.5176	0.02074	-74.85243	-11.94757
Pioglitazone vs Cloxiquine	431.25	6.5176	2.31635E-5	399.79757	462.70243
Rosiglitazone vs Cloxiquine	474.65	6.5176	1.55595E-5	443.19757	506.10243

Supplement B

BCL-x

ANOVA result: F = 436.4834, p = 0.03045

Descriptive Statistics

Treatment Group	Mean	Standard Error (SE)	95% CI Lower	95% CI Upper
BHG16 Control	390.84	36.27869	-70.12838	851.80051
Fenofibrate	369.02	7.26199	276.74771	461.29229
Agrimol B	124.97	2.5	93.20001	156.73103
DG172 dihydrochloride	193.96	10.59483	59.33685	328.57695

Pairwise Comparisons

Comparison	Mean Difference	Std. Error	p-value	95.00% LCL	95.00% UCL
Control vs Fenofibrate	21.81607	23.39265	0.79315	-91.07145	134.70358
Control vs Agrimol B	265.87055	23.39265	0.00445	152.98303	378.75806
Control vs DG172 dihydrochloride	196.87917	23.39265	0.01066	83.99166	309.76668
Fenofibrate vs Agrimol B	244.05448	23.39265	0.00572	131.16697	356.942
Fenofibrate vs DG172 dihydrochloride	175.0631	23.39265	0.01491	62.17559	287.95062
Agrimol B vs DG172 dihydrochloride	-68.99138	23.39265	0.1668	-181.87889	43.89613

CapG

ANOVA result: F = 641.85569, p = 0.02512

Descriptive Statistics

Treatment Group	Mean	Standard Error (SE)	95% CI Lower	95% CI Upper
BHG16 Control	123.11475	11.09836	-17.90329	264.1328
Fenofibrate	318.94	9.99849	191.89714	445.98286
Agrimol B	177.67241	0.32759	173.51004	181.83479
DG172 dihydrochloride	148.23276	8.88793	35.30089	261.16463

Pairwise Comparisons

Comparison	Mean Difference	Std. Error	p-value	95.00% LCL	95.00% UCL
Control vs Fenofibrate	-195.82525	6.95395	3.01376E-4	-229.38341	-162.26709
Control vs Agrimol B	-54.55766	6.95395	0.01304	-88.11582	-20.9995
Control vs DG172 dihydrochloride	-25.118	6.95395	0.10437	-58.67616	8.44016
Fenofibrate vs Agrimol B	141.26759	6.95395	7.98803E-4	107.70943	174.82575
Fenofibrate vs DG172 dihydrochloride	170.70724	6.95395	4.54205E-4	137.14908	204.2654
Agrimol B vs DG172 dihydrochloride	29.43966	6.95395	0.0703	-4.1185	62.99781

Cathepsin S

ANOVA result: F = 804.32444, p = 0.02244

Descriptive Statistics

Treatment Group	Mean	Standard Error (SE)	95% CI Lower	95% CI Upper
BHG16 Control	275.04918	5.39344	206.51899	343.57937
Fenofibrate	263	11.36321	118.61678	407.38322
Agrimol B	162.33621	9.81897	37.57442	287.09799
DG172 dihydrochloride	372.7931	22.05172	92.59938	652.98683

Pairwise Comparisons

Comparison	Mean Difference	Std. Error	p-value	95.00% LCL	95.00% UCL
Control vs Fenofibrate	12.04918	15.97764	0.87041	-65.05521	89.15357
Control vs Agrimol B	112.71297	15.97764	0.01763	35.60858	189.81737
Control vs DG172 dihydrochloride	-97.74392	15.97764	0.02627	-174.84832	-20.63953
Fenofibrate vs Agrimol B	100.66379	15.97764	0.02421	23.5594	177.76819
Fenofibrate vs DG172 dihydrochloride	-109.7931	15.97764	0.01899	-186.8975	-32.68871

Agrimol B vs DG172 dihydrochloride	-210.4569	15.97764	0.00289	-287.56129	-133.3525

DLL1

ANOVA result: F = 786.03542, p = 0.0227

Descriptive Statistics

Treatment Group	Mean	Standard Error (SE)	95% CI Lower	95% CI Upper
BHG16 Control	476.40164	24.9918	158.85067	793.95261
Fenofibrate	385.89	36.1473	-73.40498	845.18498
Agrimol B	132.27586	2.7069	97.88148	166.67024
DG172 dihydrochloride	502.75	5.02586	438.89037	566.60963

Pairwise Comparisons

Comparison	Mean Difference	Std. Error	p-value	95.00% LCL	95.00% UCL
Control vs Fenofibrate	90.51164	28.87611	0.14557	-48.83781	229.86109
Control vs Agrimol B	344.12578	28.87611	0.00388	204.77632	483.47523
Control vs DG172 dihydrochloride	-26.34836	28.87611	0.80235	-165.69781	113.00109
Fenofibrate vs Agrimol B	253.61414	28.87611	0.00943	114.26468	392.96359
Fenofibrate vs DG172 dihydrochloride	-116.86	28.87611	0.07881	-256.20945	22.48945
Agrimol B vs DG172 dihydrochloride	-370.47414	28.87611	0.00312	-509.82359	-231.12468

Enolase 2

ANOVA result: F = 2563.45981, p = 0.01257

Descriptive Statistics

Treatment Group	Mean	Standard Error (SE)	95% CI Lower	95% CI Upper
BHG16 Control	702.30328	29.7459	324.35	1080.26
Fenofibrate	423.8	10.81873	286.33	561.27
Agrimol B	744.23276	19.12931	501.17	987.29

DG172 dihydrochloride	772.27586	7.5	676.98	867.57

Pairwise Comparisons

Comparison	Mean Difference	Std. Error	p-value	95.00% LCL	95.00% UCL
Control vs Fenofibrate	278.50328	22.25597	0.00336	171.10111	385.90545
Control vs Agrimol B	-41.92948	22.25597	0.3892	-149.33165	65.47269
Control vs DG172 dihydrochloride	-69.97258	22.25597	0.14457	-177.37476	37.42959
Fenofibrate vs Agrimol B	-320.43276	22.25597	0.00222	-427.83493	-213.03059
Fenofibrate vs DG172 dihydrochloride	-348.47586	22.25597	0.00173	-455.87804	-241.07369
Agrimol B vs DG172 dihydrochloride	-28.0431	22.25597	0.6386	-135.44528	79.35907

EpCAM/TROP1

ANOVA result: F = 27735.94137, p = 0.00382

Descriptive Statistics

Treatment Group	Mean	Standard Error (SE)	95% CI Lower	95% CI Upper
BHG16 Control	410.30328	34.18852	-24.10311	844.70967
Fenofibrate	380.53	2.48902	348.90405	412.15595
Agrimol B	439.57759	13.18103	272.09666	607.05851
DG172 dihydrochloride	654.4569	29.83621	275.35194	1033.56185

Pairwise Comparisons

Comparison	Mean Difference	Std. Error	p-value	95.00% LCL	95.00% UCL
Control vs Fenofibrate	29.77328	38.35767	0.86149	-155.33201	214.87856
Control vs Agrimol B	-29.27431	38.35767	0.86677	-214.37959	155.83098
Control vs DG172 dihydrochloride	-244.15362	38.35767	0.02353	-429.2589	-59.04833

Fenofibrate vs Agrimol B	-59.04759	38.35767	0.51531	-244.15287	126.0577
Fenofibrate vs DG172 dihydrochloride	-273.9269	38.35767	0.01703	-459.03218	-88.82161
Agrimol B vs DG172 dihydrochloride	-214.87931	38.35767	0.03347	-399.9846	-29.77402

ErbB3/Her3

ANOVA result: F = 1171.11517, p =0.0186

Descriptive Statistics

Treatment Group	Mean	Standard Error (SE)	95% CI Lower	95% CI Upper
BHG16 Control	216.9918	16.48361	7.54772	426.43588
Fenofibrate	96.86	5.43765	27.76809	165.95191
Agrimol B	130.86207	3.62069	84.85684	176.86729
DG172 dihydrochloride	377.58621	9.36207	258.62984	496.54257

Pairwise Comparisons

Comparison	Mean Difference	Std. Error	p-value	95.00% LCL	95.00% UCL
Control vs Fenofibrate	120.1318	13.107	0.00833	56.88043	183.38318
Control vs Agrimol B	86.12973	13.107	0.02153	22.87836	149.38111
Control vs DG172 dihydrochloride	-160.5944	13.107	0.00357	-223.84578	-97.34303
Fenofibrate vs Agrimol B	-34.00207	13.107	0.21887	-97.25344	29.24931
Fenofibrate vs DG172 dihydrochloride	-280.72621	13.107	6.82339E-4	-343.97758	-217.47483
Agrimol B vs DG172 dihydrochloride	-246.72414	13.107	0.001	-309.97551	-183.47276

p27/Kip1

ANOVA result: F = 1554426.31732, p = 5.10617E-4

Descriptive Statistics

Treatment Group	Mean	Standard Error (SE)	95% CI Lower	95% CI Upper
BHG16 Control	144.54918	5.33607	76.74804	212.35032
Fenofibrate	131.28	1.8809	107.38085	155.17915
Agrimol B	292.18966	3.2069	251.44217	332.93714
DG172 dihydrochloride	160.68103	0.33621	156.40912	164.95295

Pairwise Comparisons

Comparison	Mean Difference	Std. Error	p-value	95.00% LCL	95.00% UCL
Control vs Fenofibrate	13.26918	5.31182	0.2361	-12.36446	38.90282
Control vs Agrimol B	-147.64047	5.31182	3.13386E-4	-173.27411	-122.00684
Control vs DG172 dihydrochloride	-16.13185	5.31182	0.15631	-41.76549	9.50179
Fenofibrate vs Agrimol B	-160.90966	5.31182	2.4226E-4	-186.54329	-135.27602
Fenofibrate vs DG172 dihydrochloride	-29.40103	5.31182	0.03459	-55.03467	-3.7674
Agrimol B vs DG172 dihydrochloride	131.50862	5.31182	4.42825E-4	105.87498	157.14226

Serpin B5/Maspin

ANOVA result: F = 5304.03634, p =0.00874

Descriptive Statistics

Treatment Group	Mean	Standard Error (SE)	95% CI Lower	95% CI Upper
BHG16 Control	586.33607	18.07377	356.68704	815.98509
Fenofibrate	479.51	36.47257	16.08209	942.93791
Agrimol B	380.55172	19.77586	129.27557	631.82788
DG172 dihydrochloride	432.31897	8.97414	318.29173	546.3462

Pairwise Comparisons

Comparison	Mean Difference	Std. Error	p-value	95.00% LCL	95.00% UCL
Control vs Fenofibrate	106.82607	36.16782	0.16626	-67.71148	281.36361

Control vs Agrimol B	205.78434	36.16782	0.03208	31.24679	380.32189
Control vs DG172 dihydrochloride	154.0171	36.16782	0.06925	-20.52045	328.55465
Fenofibrate vs Agrimol B	98.95828	36.16782	0.19603	-75.57927	273.49582
Fenofibrate vs DG172 dihydrochloride	47.19103	36.16782	0.61787	-127.34651	221.72858
Agrimol B vs DG172 dihydrochloride	-51.76724	36.16782	0.5611	-226.30479	122.77031

Survivin

ANOVA result: F = 101019.5193, p = 0.002

Descriptive Statistics

Treatment Group	Mean	Standard Error (SE)	95% CI Lower	95% CI Upper
BHG16 Control	760.06557	0.21311	757.35769	762.77345
Fenofibrate	634.71	5.12652	569.57133	699.84867
Agrimol B	204.22414	4.55172	146.389	262.05928
DG172 dihydrochloride	542.56034	7.52586	446.9352	638.18549

Pairwise Comparisons

Comparison	Mean Difference	Std. Error	p-value	95.00% LCL	95.00% UCL
Control vs Fenofibrate	125.35557	7.84574	0.00163	87.49384	163.21731
Control vs Agrimol B	555.84144	7.84574	1.72907E-5	517.9797	593.70317
Control vs DG172 dihydrochloride	217.50523	7.84574	3.15824E-4	179.64349	255.36697
Fenofibrate vs Agrimol B	430.48586	7.84574	4.07502E-5	392.62412	468.3476
Fenofibrate vs DG172 dihydrochloride	92.14966	7.84574	0.00404	54.28792	130.01139
Agrimol B vs DG172 dihydrochloride	-338.33621	7.84574	8.40659E-5	-376.19794	-300.47447